

larger in the ring compounds. With increasing temperature, however, the differences between the three polymers increase in the direction suggested by the  $\alpha_1$  values in Table V. It is reasonable to associate this difference between the two types of polymers to differences in packing and in cohesive energy density.

As has already been noted, the differences in  $\alpha_1 T_g$  simply reflect those in  $T_g$ . The constancy of  $\Delta\alpha T_g$  suggests that the side-chain effects which have been invoked to rationalize smaller numerical values in the *n*-alkyl methacrylate series,<sup>15</sup> either are not operative, or affect both the liquid and the glassy state in the two ring polymers. In contrast, the free volume integral is sensitive to the relax-

ational activity in the glass, as monitored by the last integral in Table V, with the value of the former being unusually large for I-PMMA. While the numerical values of the other quantities ultimately reflect structural differences, it is noteworthy to contrast this once again with the characteristic constancy of the product  $\Delta\alpha T_g$ .

In the following paper we will examine these and additional experimental results in the liquid and glassy states from the point of view of a theoretical equation of state.

**Acknowledgment.** We thank the National Science Foundation for support under Grants GK-20653 and GH-36124.

## Thermal Expansion of Amorphous Polymers at Atmospheric Pressure. II. Theoretical Considerations

Robert Simha and Phillip S. Wilson\*

Department of Macromolecular Science, Case Western Reserve University, Cleveland, Ohio 44106.  
Received July 30, 1973

**ABSTRACT:** We analyze a number of structurally diverse systems. A simple interpolation expression represents accurately the implicit form of the theoretical equation of state for the liquid derived previously, and facilitates numerical evaluations. The very good agreement between predicted and measured volumes is in accord with earlier observations. Thermal expansivities,  $\alpha$ , are estimated with a maximum error, averaged over all systems investigated, of 3.7%. The theoretical temperature dependence of  $\alpha$  is  $\propto T^{1/2}$ . However, the experimental results are better approximated by a linear function or by a proportionality factor which decreases with increasing  $T$ . The volume and temperature scaling parameters are compared for different polymers. The characteristic temperature  $T^*$  shows a parallel trend with  $T_g$ . But, not surprisingly,  $T_g$  is not strictly a corresponding temperature. Hence the hole fraction  $1 - \gamma$  at  $T_g$  is not constant, but increases with increasing reduced, and essentially actual glass temperature. A connection between the liquid and glassy states is provided by the temperature dependence of  $\gamma$ , finite also in the glass, as shown earlier, and treated there as an adjustable quantity in the theoretical equation of state. From the difference between the experimental and theoretical  $\gamma$ 's for the glass and supercooled liquid, respectively, a characteristic frozen fraction can be deduced which increases with decreasing  $T_g$ . In accord with well-known macroscopic characteristics, the frozen fractions in the series of *n*-alkyl methacrylates are comparatively small and exhibit a minimum as a function of side-chain length.

We have previously shown the close agreement between master curves constructed from volume-temperature data at atmospheric pressure, encompassing oligomers and polymers,<sup>1</sup> and the predictions of our hole theory.<sup>2</sup> Such comparisons were subsequently extended to detailed data from our laboratory, including elevated pressures for polystyrene and poly(*o*-methylstyrene).<sup>3</sup> Finally, some high-pressure results taken from the literature, were also discussed.<sup>4</sup> The quantitative success of the theory has enabled us to proceed to the liquid-glass transition region and finally to explore the glassy state in terms of theoretical results, developed originally for the liquid equilibrium state.<sup>3,5,6</sup>

We are now in a position to investigate in detail the volume-temperature relations for series of structurally related as well as widely different polymers. This program is pursued here only at atmospheric pressure. Thus we obtain the specific characteristic volume ( $V^*$ ) and temperature ( $T^*$ ) scaling factors and define in quantitative detail the performance of the theory. Secondly, we examine the behavior of the hole fraction as a characteristic ordering parameter, in the glassy state of these polymers with their

widely differing glass temperatures, and obtain semiempirical relationships. The accuracy of the experimental data with their different origins is not uniform. Nevertheless, the nature of our conclusions, as will be seen, is not affected by these differences.

Table I lists in order of decreasing  $T_g$ , except for the alkyl methacrylate series, the systems to be investigated and the sources of data.<sup>3,7-19</sup> These include earlier results from this laboratory and those reported in the foregoing paper<sup>9</sup> to which we added measurements<sup>12</sup> on a high mo-

(1) R. Simha and A. J. Havlik, *J. Amer. Chem. Soc.*, **86**, 197 (1964).

(2) R. Simha and T. Somcynsky, *Macromolecules*, **2**, 342 (1969).

(3) A. Quach and R. Simha, *J. Appl. Phys.*, **42**, 4592 (1971); *Macromolecules*, **4**, 268 (1971).

(4) R. Simha, P. S. Wilson, and O. Olabisi, *Kolloid-Z. Z. Polym.*, in press.

(5) T. Somcynsky and R. Simha, *J. Appl. Phys.*, **42**, 4545 (1971).

(6) A. Quach and R. Simha, *J. Phys. Chem.*, **76**, 416 (1972).

(7) J. M. G. Cowie and P. M. Toporowski, *J. Macromol. Sci., Phys.*, **1**, 81 (1969).

(8) J. P. Mercier, J. J. Aklonis, M. Litt, and A. V. Tobolsky, *J. Appl. Polym. Sci.*, **9**, 447 (1965).

(9) P. S. Wilson and R. Simha, *Macromolecules*, submitted for publication.

(10) S. S. Rogers and L. Mandelkern, *J. Phys. Chem.*, **61**, 985 (1957).

(11) K. H. Hellwege, W. Knappe, and P. Lehmann, *Kolloid-Z. Z. Polym.*, **183**, 110 (1962).

(12) P. S. Wilson, Ph.D. Thesis, Case Western Reserve University, 1973.

(13) L. Mandelkern, G. M. Martin, and F. A. Quinn, *J. Res. Nat. Bur. Stand., Sect. A*, **58**, 137 (1957).

(14) J. E. McKinney, National Bureau of Standards, U. S., private communication.

(15) M. Takahishi, M. C. Shen, R. B. Taylor, and A. V. Tobolsky, *J. Appl. Polym. Sci.*, **8**, 1549 (1964).

(16) G. Kraus and J. T. Gruver, *J. Polym. Sci., Part A-2*, **8**, 571 (1970).

(17) B. E. Eichinger and P. J. Flory, *Macromolecules*, **1**, 285 (1968).

(18) H. Shih and P. J. Flory, *Macromolecules*, **5**, 758 (1972).

(19) K. Polmanteer, Dow Corning Corp., Midland, Mich., private communication.

Table I  
List of Systems Studied

Abbrev	Polymer of	Ref
1. PaMS(a)	$\alpha$ -Methylstyrene (95% syndiotactic)	7
2. PaMS(b)	$\alpha$ -Methylstyrene (67% syndiotactic)	7
3. PCarb	Carbonate of bis(phenol A)	8
4. PoMS	<i>o</i> -Methylstyrene	3
5. PCHMA	Cyclohexyl methacrylate	9
6. A-PMMA(a)	Atactic methyl methacrylate	10
7. A-PMMA(b)	Atactic methyl methacrylate	11
8. A-PMMA(c)	Atactic methyl methacrylate	12
9. PEMA	Ethyl methacrylate	10
10. PnPMA	<i>n</i> -Propyl methacrylate	10
11. PnBMA	<i>n</i> -Butyl methacrylate	10
12. PnHMA	<i>n</i> -Hexyl methacrylate	10
13. PnOMA	<i>n</i> -Octyl methacrylate	10
14. PnDMA	<i>n</i> -Dodecyl methacrylate	10
15. PnODMA	<i>n</i> -Octadecyl methacrylate	10
16. PS(a)	Styrene	12
17. PS(b)	Styrene	11
18. PS(c)	Styrene	3
19. PVC	Vinyl chloride	11
20. PCPMA	Cyclopentyl methacrylate	9
21. I-PMMA	Isotactic methyl methacrylate	9
22. PCIF <sub>3</sub> E	Chlorotrifluoroethylene	13
23. PVAc	Vinyl acetate	14
24. PMA	Methyl acrylate	15
25. SBR	Styrene–butadiene	16
26. PIB	Isobutylene	17
27. PDMSi(a)	Dimethylsiloxane	18
28. PDMSi(b)	Dimethylsiloxane	19
29. HMW-PE	Ethylene	12
30. C <sub>22</sub> H <sub>46</sub>	Oligomer of methylene	9

lecular weight linear polyethylene, furnished by Allied Chemical Corp., their designation 260-100.

### I. Theoretical Relationships and Liquid State Results

The reduced equation of state at atmospheric pressure assumes the form<sup>2</sup>

$$\tilde{T} = 2y(y\tilde{V})^{-2}[1.2045 - 1.011(y\tilde{V})^{-2}][1 - 2^{-1/6}y(y\tilde{V})^{-1/3}] \quad (1)$$

The condition on the vacancy fraction  $1 - y$  for an infinite smer with one external degree of freedom per segment,  $3c/s = 1$ , is given by the equation

$$1 + y^{-1} \ln(1 - y) = (y/6\tilde{T})(y\tilde{V})^{-2}[2.409 - 3.033(y\tilde{V})^{-2}] + [2^{-1/6}y(y\tilde{V})^{-1/3} - (1/3)][1 - 2^{-1/6}y(y\tilde{V})^{-1/3}]^{-1} \quad (2)$$

We have shown that eq 1 and 2 can in very good approximation be replaced by the interpolation expression<sup>4</sup>

$$\ln \tilde{V} = -0.1033_5 + 23.834_5 \times \tilde{T}^{3/2} \quad 1.65 < \tilde{T} \times 10^2 < 7.03 \quad (3)$$

where

$$\tilde{\alpha} = 35.751_8 \times \tilde{T}^{1/2} \quad (4)$$

and

$$\ln \tilde{V} = -0.1033_5 + (2/3)\alpha T \quad \alpha T = 35.751_8 \times \tilde{T}^{3/2} \quad (3a)$$

For the evaluation of the primary quantities, eq 3, 3a, and 4 are more convenient to use and more transparent than the original expressions 1 and 2. Two general procedures are employed. In one, the experimental data in double-logarithmic form are superimposed on the theoretical

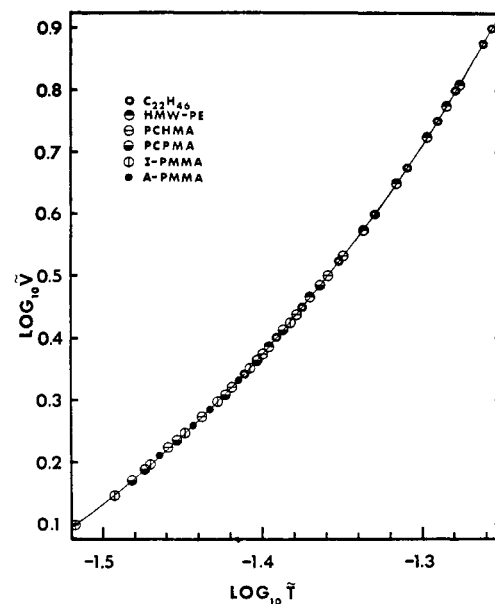


Figure 1. Theoretical master curve and superimposed experimental data.

reduced isobar where average or smoothed  $V^*$  and  $T^*$  are derived. The typical result is illustrated for our most recent data in Figure 1. The oligomer aids in extending the temperature range and this plot once more illustrates the kind of agreement we obtain. A more stringent test of the derivatives is provided by a combination of relations 3a and 3. Substitution of experimental values for  $V$  and  $\alpha T$  in the first equation (3a) over the whole temperature range yields a point by point determination of  $V^*$ . Substitution into eq 3 then provides a point by point determination of  $T^*$ .

For theoretical reasons and extensions to the glassy state, it is necessary to have explicit results for the temperature dependence of  $y$  (eq 2). These were tabulated in the original paper<sup>2</sup> only for the range appropriate for liquid argon and therefore are displayed in Table II.<sup>20</sup> For future reference we include the last column which represents the slope of the  $y$ - $\tilde{T}$  function (see Figures 3–5) in the pertinent temperature range. We note again the relative constancy of the cell volume ( $y\tilde{V}$ ) which varies only from 0.947 to 0.967, when  $\tilde{V}$  changes by about 31% and  $\tilde{T}$  by a factor of 4. A constant ( $y\tilde{V}$ ) would imply validity of van der Waals' form for the internal energy.<sup>2</sup>

By means of the superposition procedure described above, we obtain the numerical values of the scaling factors, displayed in Table III. We recall that the evaluation of the segmental characteristic volume requires pressure data<sup>4</sup> and hence only specific volumes  $V^*$  can be quoted here. It is nevertheless of interest to make some comparisons between different systems, although there are slight differences for the same polymer between different investigators. The polystyrene group has relatively large  $V^*$ 's, with the *o*-methyl having a larger and the  $\alpha$ -methyl a smaller value than normal styrene. The pressure results<sup>3,21</sup> show that the segmental volumes are practically identical for the first and third. No information regarding the second is available. In the methacrylate series we note the expected monotonic increase with increasing length of the side chain. Noteworthy is the difference between atactic ( $\approx 0.84$ ) and isotactic ( $\approx 0.82$ ) PMMA. We have earlier commented on the tighter packing in the stereoregular

(20) T. Somcynsky, unpublished data.

(21) O. Olabisi, Ph.D. Thesis, Case Western Reserve University, 1973.

Table II  
Solution of Equations 1 and 2 for Incremental Reduced  
Volume Changes of 0.01

$\bar{V}$	$\bar{T} \times 10^2$	$(1 - \gamma) \times 10^2$	$\gamma \bar{V}$	$(d\gamma/d\bar{T})_1$
0.95	1.6531	0.2816	0.947324	
0.96	1.9115	1.0297	0.950115	3.6285
0.97	2.1206	1.9090	0.951483	4.5068
0.98	2.3105	2.8200	0.952364	4.9584
0.99	2.4891	3.7350	0.953023	5.2215
1.00	2.6598	4.6437	0.953563	5.3948
1.01	2.8240	5.5414	0.954032	5.5176
1.02	2.9828	6.4258	0.954457	5.6132
1.03	3.1366	7.2958	0.954853	5.6881
1.04	3.2861	8.1510	0.955229	5.7518
1.05	3.4314	8.9912	0.955592	5.8076
1.06	3.5729	9.8165	0.955945	5.8547
1.07	3.7108	10.6269	0.956292	5.8966
1.08	3.8453	11.4227	0.956634	5.9347
1.09	3.9766	12.2043	0.956974	5.9660
1.10	4.1049	12.9718	0.957311	6.0025
1.11	4.2301	13.7255	0.957647	6.0286
1.12	4.3526	14.4659	0.957982	6.0571
1.13	4.4724	15.1932	0.958317	
1.14	4.5896	15.9077	0.958652	
1.15	4.7043	16.6098	0.958988	
1.16	4.8166	17.2997	0.959324	
1.17	4.9266	17.9777	0.959661	
1.18	5.0343	18.6442	0.959999	
1.19	5.1399	19.2994	0.960338	
1.20	5.2435	19.9435	0.960677	
1.21	5.3450	20.5770	0.961018	
1.22	5.4445	21.2000	0.961360	
1.23	5.5422	21.8127	0.961704	
1.24	5.6380	22.4155	0.962048	
1.25	5.7320	23.0085	0.962394	
1.26	5.8243	23.5920	0.962741	
1.27	5.9150	24.1663	0.963089	
1.28	6.0040	24.7314	0.963438	
1.29	6.0914	25.2877	0.963788	
1.30	6.1773	25.8354	0.964140	
1.31	6.2617	26.3746	0.964493	
1.32	6.3447	26.9056	0.964846	
1.33	6.4262	27.4285	0.965202	
1.34	6.5064	27.9434	0.965558	
1.35	6.5852	28.4507	0.965915	
1.36	6.6626	28.9505	0.966274	
1.37	6.7389	29.4428	0.966633	

system.<sup>22</sup> The segmental volume factor also turns out to be smaller for I-PMMA.<sup>22</sup> The characteristic ratio  $3c/s$  is assumed fixed here and the magnitude of the segmental molecular weight characterizes the unit required to satisfy this condition. Hence the smaller value for I-PMMA may be taken as a reflection of enhanced flexibility.<sup>22</sup>

Owing to the assumption regarding  $3c/s$ ,  $T^*$  is a direct measure of the segmental interaction energy. It is not surprising therefore that no significant differences within the styrene group are found. The systematic decrease in the alkyl methacrylate series correlates with the reduced polarity and increased hydrocarbon character. Pressure data show that the characteristic segmental volume of PnBMA is not larger than that of atactic PMMA.<sup>21</sup> The strong interactions between the side chains in PnODMA are evidenced not only by the appearance of a melting transition,<sup>10</sup> but also by the large value of  $T^*$ . The difference

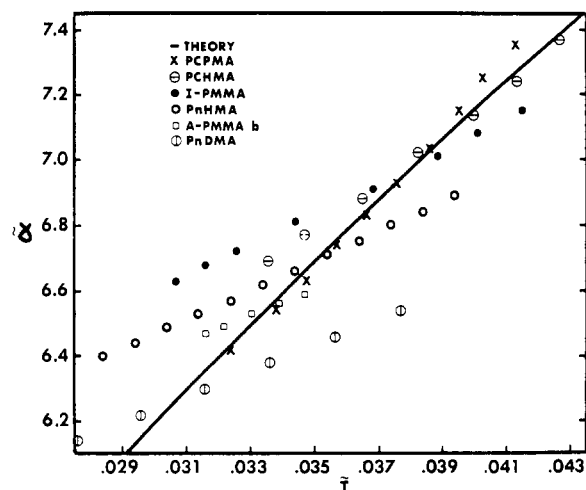


Figure 2. Thermal expansivity as a function of temperature in reduced coordinates.

between the two PMMA species is consistent with a suggested association between isotactic and syndiotactic sequences.<sup>23</sup>

Finally we compare the high molecular weight polyethylene with *n*-docosane. The analysis of Simha and Havlik leads to the relation<sup>1</sup>

$$T^*(n) = T^*(\infty)[1 - 5.6/(n + 7)]$$

with the result  $T^*(n = 22) = 7840^\circ\text{K}$ , compared with the observed  $8340^\circ\text{K}$ . Moreover<sup>1</sup>

$$V^*(n) = V^*(\infty)[1 + 5.0207/(7n + 1)]$$

or  $V^*(n = 22) = 1.1776$  vs. the observed 1.1905. Actually the characteristic parameters of the *n*-paraffins do not extrapolate smoothly to the values for this particular polyethylene sample.<sup>21</sup> We note that an extrapolation of the amorphous alkyl methacrylate series to  $n = \infty$  results in a  $T^*$  about intermediate between those for the two hydrocarbons.

The last column in Table III shows the temperature ranges available, always starting from  $T_g$  (or  $T_m$ ) + 10. By means of the point-by-point evaluation procedure, the third and fifth columns are obtained. The variations  $\Delta V^*$  and  $\Delta T^*$  have for purposes of comparison been normalized to 100°, although they are not strictly linear. We note that both  $V^*$  and  $T^*$  increase with  $T$ . The percentage variations are tabulated as the difference between the maximum and minimum value, divided by the latter. The averaged normalized variation in  $T^*$  amounts to 5.2% with a maximum of 8.2%. For  $V^*$  the corresponding values are 1.1 and 2.4%, respectively. The consequences of these variations for the predicted specific volume and thermal expansivity are also presented. The maximum error in the former, 1.16%, occurs for one of the polystyrenes. This exceeds considerably the other deviations, including even those for the long-chain methacrylates. The average maximum deviation between computed and experimental volumes is only 0.31%. The maximum in respect to  $\alpha$  is 9.8% (PIB), with the mean maximum being 3.7%.

Figure 2 illustrates the relation between the reduced experimental and theoretical thermal expansivities as a function of reduced temperature for some typical systems. While the numerical agreement is gratifying, the theory exaggerates the temperature dependence of  $\alpha$  (see eq 4).

(22) A. Quach, P. S. Wilson, and R. Simha, *J. Macromol. Sci.*, in press; *Polym. Prepr., Amer. Chem. Soc., Div. Polym. Chem.*, in press.

(23) W. Borchard, M. Pyrlík, and G. Rehage, *Makromol. Chem.*, **145**, 169 (1971).

Table III  
Liquid-State Theoretical Quantities<sup>a</sup>

Material	$T^*$ (°K)	$\Delta T^*/100^\circ$ (%)	$V^*$ (cm <sup>3</sup> /g)	$\Delta V^*/100^\circ$ (%)	Max $V_{sp}$ Error (%)	Max $\alpha$ Error (%)	$\Delta T_1$ (°K)
PS(a)	11800	6.50	0.9470	1.70	1.16	6.60	120
PS(b)	12700	4.08	0.9625	0.88	0.48	4.32	130
PS(c)	12680	4.49	0.9598	0.96	0.22	3.82	80
PoMS	12740	4.07	0.9762	0.93	0.07	3.88	70
P $\alpha$ MS(a)	12790	3.32	0.9231	0.90	0.63	4.06	40
P $\alpha$ MS(b)	12700	3.48	0.9152	0.81	0.52	2.89	45
A-PMMA(a)	11910	4.65	0.8433	1.19	0.22	1.13	30
A-PMMA(b)	11890	4.87	0.8350	0.93	0.15	1.19	30
A-PMMA(c)	11940	8.63	0.8362	1.97	0.05	2.09	30
<hr/>							
PEMA	11540	5.28	0.8862	1.08	0.22	1.80	40
PnPMA	10890	5.46	0.9238	1.13	0.04	3.33	70
PnBMA	10540	5.40	0.9415	1.06	0.52	3.61	90
PnHMA	9980	5.68	0.9727	1.20	0.77	5.90	110
PnOMA	9770	6.36	1.0058	0.42	0.55	4.77	120
PnDMA	9190	6.40	1.0387	1.11	0.82	7.63	140
PnODMA	11360	5.91	1.1576	1.13	0.51	3.70	80
<hr/>							
I-PMMA	11170	4.57	0.8160	0.99	0.12	6.40	130
PCPMA	10740	2.43	0.8730	0.73	0.13	3.66	120
PCHMA	11320	1.31	0.8910	0.39	0.08	1.50	100
HMW-PE	9710	1.74	1.1406	0.63	0.30	1.47	90
C <sub>22</sub> H <sub>46</sub>	8340	5.02	1.1905	0.35	0.09	1.70	150
PVC	11320	4.93	0.7105	1.18	0.33	3.08	30
PVAc	9410	8.52	0.8140	2.05	0.29	2.19	55
PMA	9200	5.95	0.7925	1.33	0.36	2.59	50
SBR	9800	6.20	0.9892	1.35	0.04	2.77	40
PIB	11220	8.17	1.0902	1.51	0.14	9.80	150
PDMSi(a)	8160	7.19	0.9690	2.39	0.21	7.80	180
PDMSi(b)	7920	4.20	0.9594	1.24	0.14	1.80	55
PClF <sub>3</sub> E	13880	6.80	0.4852	0.98	0.05	2.21	40
PCarb	12130	3.84	0.8100	0.70	0.18	2.12	40

<sup>a</sup> Dashed line segregates *n*-alkyl methacrylate series.

Actually, for all the systems studied,  $\tilde{\alpha}$  could be approximated by a linear function in  $\tilde{T}$ . Therefore an empirical mastercurve could be constructed.

The temperature factor  $T^*$  is defined by the balance between thermal ( $\propto ckT^*$ ) and maximum attractive energy. The experimentally observed increase of the parameter  $T^*$  implies a decrease in the number of effectively external degrees of freedom with increasing temperature. For an assumed constant ratio  $c/s$ , this requires a corresponding increase in the size of the segment.

Before concluding this section, we note that a characteristic square-root dependence of  $\alpha$  (eq 3a) has been obtained on more intuitive grounds from some considerations by Bueche.<sup>24</sup> He considers a free volume in terms of holes whose size distribution is governed by a Boltzmann factor in the surface energy. Recently Litt<sup>25</sup> has taken up this subject. Expressing the volume as a linear function of the free volume fraction, the thermal expansivity can be cast in the following form

$$\alpha T = (3/2)\tilde{T}^{3/2}/(1 + \tilde{T}^{3/2}) \quad (5)$$

$$\tilde{V} = [1 - (2/3)\alpha T]^{-1}$$

with, of course, a different definition of the scale factors.

Table IV  
Comparison of S-S and B-L Results<sup>a</sup>

	Max. $\alpha$ Error (%)		$\Delta T^*/100^\circ$ (%)		$\Delta V^*/100^\circ$ (%)	
	S-S	B-L	S-S	B-L	S-S	B-L
PIB	9.80	6.13	8.17	4.68	1.51	0.86
PS	6.60	2.06	6.50	1.60	1.70	0.73
PDMSi	7.80	1.72	7.19	0.90	2.39	0.32
C <sub>22</sub> H <sub>46</sub>	1.72	7.48	5.02	9.96	0.35	3.93

<sup>a</sup> Simha-Somcynsky and Bueche-Litt.

The last equation may be compared with our expression, viz.

$$\tilde{V}' = \exp[(2/3)\alpha T] \quad (4')$$

where the prime indicates that the constant term in eq 3 has been included in the definition of the volume scaling factor. Equations 4' and 5 are identical up to terms  $O(\alpha T)$ , but for higher temperatures eq 5 predicts a slower variation of  $\alpha$  with  $T$ , in qualitative accord with Figure 2. Table IV shows numerical results for some liquid systems with large  $\Delta T_1$ . With the exception of the oligomer, the agreement is better and the variations in the scaling parameters are smaller than in the theory. But, as we have said on other occasions, numerical agreement in respect to

(24) F. Bueche, "Physical Properties of Polymers," Interscience Publishers, New York, N. Y., 1962, pp 85–110.

(25) M. Litt, *Polym. Prepr., Amer. Chem. Soc., Div. Polym. Chem.*, **14**, 109 (1973).

Table V  
Glassy-State Theoretical Questions<sup>a</sup>

Polymer	$T_g$ (°K)	$T^* \times 10^{-4}$ (°K)	$T_g \times 10^2$	$(1 - y_g)$ $\times 10^2$	$(\Delta y / \Delta T)_g$ $\times (10^4 / ^\circ\text{K})$	$f$
PαMS(a)	455	1.279	3.559	9.74	2.47	0.460
PαMS(b)	448	1.270	3.528	9.56	2.38	0.483
PCarb	423	1.213	3.488	9.32	1.92	0.530
PoMS	404	1.274	3.171	7.49	1.82	0.594
PCHMA	380	1.132	3.357	8.55	2.46	0.518
A-PMMA(a)	378	1.191	3.176	7.51	1.80	0.624
A-PMMA(b)	376	1.189	3.162	7.42	1.77	0.629
A-PMMA(c)	373	1.194	3.124	7.22	1.77	0.630
<hr/>						
PEMA	338	1.154	2.930	6.14	1.89	0.610
PnPMA	308	1.089	2.828	5.58	2.64	0.480
PnBMA	293	1.054	2.783	5.32	3.35	0.358
PnHMA	268	0.998	2.686	4.79	4.57	0.159
PnOMA	253	0.977	2.591	4.26	3.25	0.404
PnDMA	208	0.919	2.265	2.59	1.13	0.786
<hr/>						
PS(a)	369	1.180	3.127	7.23	1.99	0.587
PS(b)	365	1.270	2.874	5.82	1.50	0.656
PS(c)	362	1.268	2.855	5.72	1.36	0.689
PVC	349	1.132	3.083	6.99	1.96	0.609
PCPMA	348	1.074	3.234	7.89	2.06	0.614
I-PMMA	320	1.117	2.864	5.78	1.66	0.665
PClF <sub>3</sub> E	318	1.388	2.290	2.71	0.81	0.771
PVAc	304	0.941	3.228	7.82	1.80	0.704
PMA	281	0.920	3.055	6.84	1.71	0.722
SBR	257	0.980	2.624	4.44	0.93	0.830
PDMSi(a)	150	0.816	1.838	0.98	0.23	0.950
		(0.800)	(1.875)	(0.99)	(0.80)	(0.830)

<sup>a</sup> Dashed line segregates *n*-alkyl methacrylate series.

second derivatives of a configurational partition function beyond what we have obtained here, represents a very stringent requirement. It should be noted that predictions within the limitations shown, are sufficient for most practical processing applications.

## II. Glassy-State Correlations

We extend here the approach developed and applied to polystyrene and poly(*o*-methylstyrene).<sup>6</sup> That is, we relate the glass transition and the pressure-volume-temperature (PVT) properties of a "constant formation" glass to a departure in the dependence of  $y$  on  $\bar{V}$  and  $\bar{T}$  from that predicted by the equilibrium condition (eq 2). Some time ago we demonstrated that the assumption of a constant  $y$  results in too small an  $\alpha_g$ .<sup>5,6</sup> In other words, the holes make a considerable contribution to the thermal expansion of the glass, a contribution which is practically eliminated only around 50°K or so, corresponding to reduced temperatures of considerably less than  $10^{-2}$ .<sup>26</sup> We have proceeded in a semiempirical manner by treating  $y$  as an adjustable parameter in eq 1 and its corresponding form for finite reduced pressures  $\bar{P}$ .<sup>6</sup>

We begin with the transition region. Table V lists the polymers in order of decreasing  $T_g$ , except for the methacrylate series. These are compared with the  $T^*$ , taken from Table III. Not surprisingly, a parallel trend between the two characteristic temperatures exists. However, the reduced glass temperature,  $\bar{T}$ , does not assume a universal value,  $T_g$  varying more than  $T^*$ . Generally speaking, rubbery polymers yield lower  $\bar{T}_g$ 's. The fact that  $T_g$  does not represent a corresponding temperature has been stressed

a long time ago and follows immediately from the observed variability of the product  $\alpha_1 T_g$ .<sup>27</sup> However, within groups of polymers, the variations are not too pronounced, as is evident in the column of  $\bar{T}$ 's. While  $T_g$ , determined by kinetic processes, should not strictly be a characteristic temperature in respect to equilibrium processes, it is at least approximately that. It follows immediately, that the hole fraction  $1 - y_g$  at  $T_g$  cannot be constant. Instead, it decreases with decreasing  $\bar{T}$ , which to a large extent then implies decreasing  $T_g$ . This is a physically reasonable result; low  $T_g$  systems should require relatively few holes to pass into the liquid state.

In constructing the table, an adjustment in the  $T^*$  value obtained in section I for PDMSi was necessary, owing to the large gap between  $T_g$  (150°K) and the starting temperature of the data.<sup>18</sup> In order to place this polymer on a comparable basis with the other systems analyzed,  $T^*$  was corrected by linear extrapolation to a value corresponding to the midpoint of the range from  $T_g$  to the highest temperature. This changes  $T^*$  from 8160°K (see Table III) to 8000°K and  $1 - y$  from 0.0098 to 0.0099. We note that the average observed variability in  $T^*$ , about 5%, would change  $1 - y_g$  by about 2.5%.

We continue into the glassy region. Figures 3-5 show the temperature dependence of the vacancy fraction for our three methacrylates.<sup>9</sup> It will be noted that in PCHMA, the polymer with the highest  $T_g$ , the glassy line is closest to the extrapolated liquid curve, derived from eq 2. The relationship between these two lines could be utilized to define an effective temperature,<sup>28</sup> at which a

(26) R. Simha, J. M. Roe, and V. S. Nanda, *J. Appl. Phys.*, **43**, 4312 (1972).

(27) R. Simha and R. F. Boyer, *J. Chem. Phys.*, **37**, 1003 (1962); *J. Polym. Sci., Part B*, **11**, 33 (1973).

(28) A. Q. Tool and C. G. Eichlin, *J. Amer. Ceram. Soc.*, **14**, 276 (1931).

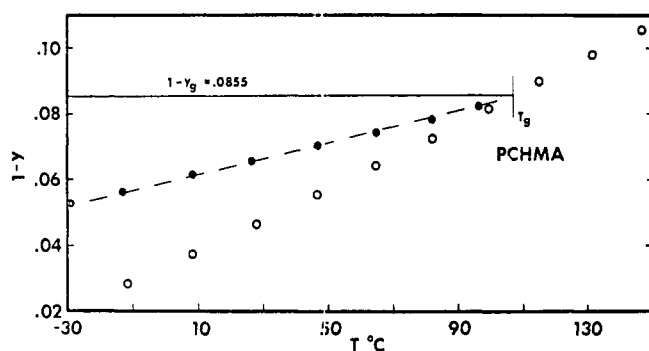


Figure 3. Hole fraction as a function of temperature for PCHMA. Solid circles, experimental; open circles, liquid, eq 1 and 2; solid line, value at  $T_g$ .

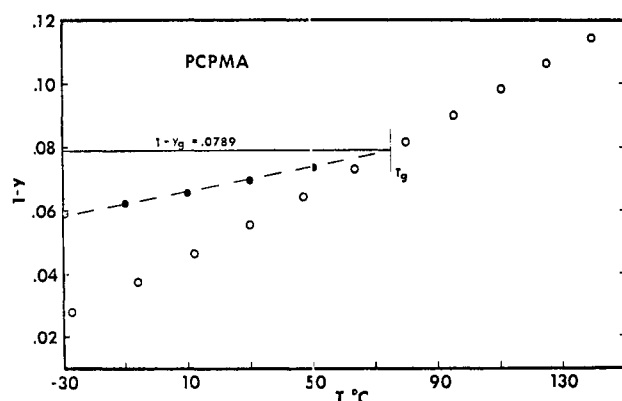


Figure 4. Hole fraction as a function of temperature for PCPMA. Solid circles, experimental; open circles, liquid, eq 1 and 2; solid line, value at  $T_g$ .

given configuration of the glass (characterized here by the parameter  $y$ ) could be observed in the corresponding equilibrium liquid. We propose to employ here an alternative characterization. By means of the differences between the two slopes, we can define a "frozen fraction"  $f$  as

$$f = 1 - [(dy/dT)_g / (dy/dT)_l] \quad (6)$$

These derivatives are strictly functions of temperature. However it will be seen that over a considerable range the first one may be taken as a constant. The second one is obtained from the last column in Table II and  $T^*$ . The  $f$  values to be quoted refer to  $T = T_g$ . It is noteworthy, that the presence of a  $\beta$  relaxation is evidenced by a second decrease in the slope of  $1 - y$ , as seen in Figure 5.

Table V lists the numerical values of  $(\Delta y / \Delta T)_g$  and  $f$ . These are sensitive to variations in  $T^*$ . The correction of 2% made for PDMSi, for example, changes  $f$  from 0.95 to 0.83. For materials of higher  $T_g$  with their larger  $1 - y_g$  and  $(dy/dT)_g$ , a 5% change in  $T^*$  leads to an approximately 10% shift in  $f$ .

In Figure 6 we illustrate the important relationships. The spread in reduced glass temperatures and  $1 - y_g$  is visible with the characteristic clustering of values; note the  $T_g$  region between about 0.028 and 0.032. The extremities are formed by PaMS, PCarb, and the siloxane. Disregarding the higher members in the series of  $n$ -alkyl methacrylates, we can draw a monotonic correlation line for the frozen fractions with limits of less than 0.5 to about 0.9. This line must tend toward unity, as  $T_g \rightarrow 0$ . The divergent loop expresses in another quantitative manner the fact that these side-chain polymers have a pronounced liquid-like character, as is reflected in their large

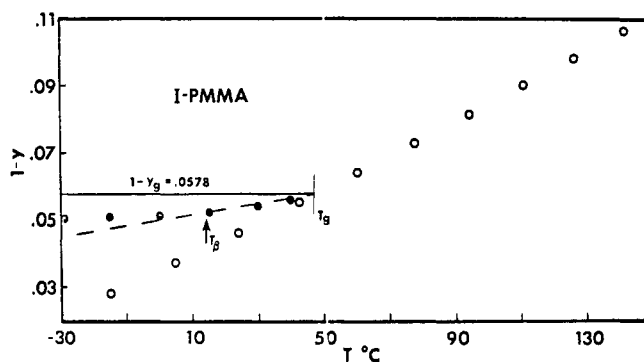


Figure 5. Hole fraction as a function of temperature for I-PMMA. Solid circles, experimental; open circles, liquid, eq 1 and 2; solid line, value at  $T_g$ .

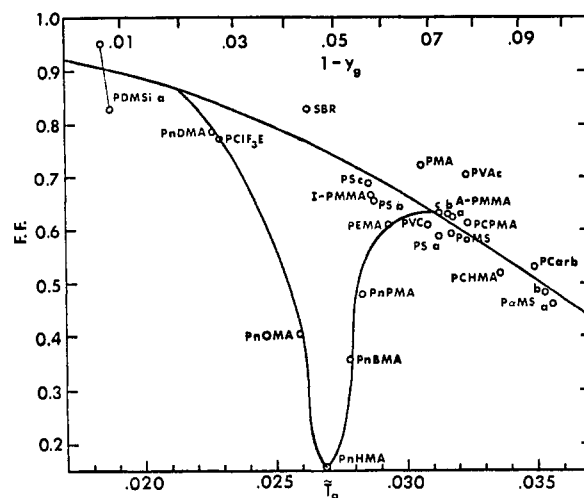


Figure 6. Correlation of frozen fraction with hole fraction at  $T_g$  and with  $T_g$ .

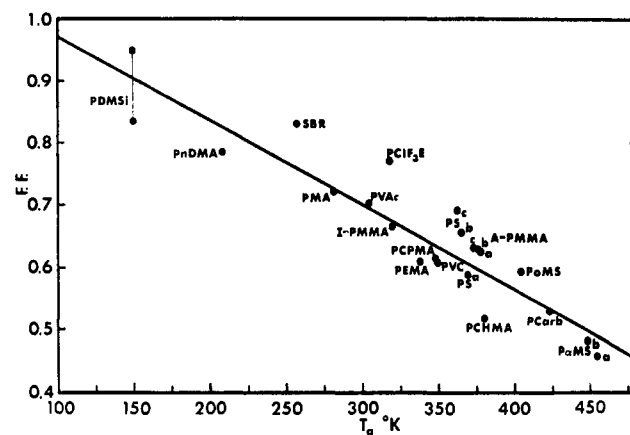


Figure 7. Correlation of frozen fraction with  $T_g$ .

thermal expansivities,<sup>27</sup> and extrema with chain length in respect to these features.

We present in Figure 7 an approximate correlation between  $f$  and  $T_g$ . The equation of the straight line is

$$f = 1.107 - 1.346 \times 10^{-3} \times T_g \quad (7)$$

The maximum deviations are +12% (PCIF<sub>3</sub>E) and -15% (PCHMA), with the C<sub>3</sub> to C<sub>8</sub> methacrylates excluded. Equation 7 is not applicable for low  $T_g$ 's since it does not have the correct limit, because  $f = 1$  for  $T_g = 82^\circ\text{K}$ .

Although the absolute values of  $f$  are very sensitive to the accuracy of the glassy data, the relative order shown here should remain valid. Figures 6 and 7 also indicate the desirability of information on systems in the range  $T_g < 300^\circ\text{K}$  and  $> 450^\circ\text{K}$ .

### III. Conclusions

The results on the diverse systems examined extend and strengthen previous conclusions. In the liquid state, the quantitative performance of the theory appears now sufficiently defined. Practically useful estimates of liquid densities can be obtained from a minimum of experimental information. The characteristic scaling parameters, in this work only  $V^*$  and  $T^*$ , which are determined from experiment, can provide more informative comparisons between different systems than the macroscopic quantities themselves. Moreover, they are a guide for the selection of additional structures for investigation. Here the pressure variable is important and future publications are to extend previous work<sup>3,22</sup> in this direction.

The extension into the glassy region by a combination of experiment and theory enables us to characterize different glasses in terms of the structural parameter  $\gamma$  and its temperature derivative, or the frozen fraction  $f$ . As is illustrated by means of the methacrylate series, these quantities sensitively monitor structural differences. As has been pointed out earlier, these results have a bearing on the phenomenological treatment of the transition process in terms of frozen ordering parameters. Here again pressure studies are important.<sup>6</sup> Densities can be estimated from the correlations presented, once  $V^*$ ,  $T^*$ , and  $T_g$  are known. Considerable fluctuations in the numerical values of  $f$  produce much smaller variations in specific volume, for example, 20 *vs.* 0.1%. Of course, the converse places a considerable strain on experimental accuracy.

While our objects of investigation have been organic polymer glasses, it will certainly be interesting to explore these quite general ideas for other types of glasses as well.

**Acknowledgment.** We thank the National Science Foundation for support under Grant GH-36124.

## Thermal Expansion and Differential Scanning Calorimetry Phenomena in the $\gamma$ -Relaxation Region ( $\approx 150^\circ\text{K}$ ) of Nylon 6,6, Nylon 11, and Ethylene-co-(Vinyl acetate)

Phillip S. Wilson,<sup>1a</sup> Shirely Lee,<sup>1a</sup> and Raymond F. Boyer\*<sup>1b</sup>

Department of Macromolecular Science, Cleveland, Ohio 44106, and the Dow Chemical Company, Midland, Michigan 48640. Received May 9, 1973

**ABSTRACT:** Linear thermal expansion coefficients,  $\alpha'$ , have been determined in the temperature range from liquid  $\text{N}_2$  to  $T_g$  for Nylon 6,6, Nylon 11, and ethylene-co-(28 wt % vinyl acetate).  $\alpha'$  shows a two- or possibly three-stage discontinuity well above experimental error for the two nylons but a less drastic increase for the copolymer. These events appear to be associated with the well-known mechanical  $\gamma$  relaxation at  $\sim 150^\circ\text{K}$  for these three polymer systems. These increases in  $\alpha'$  are much greater than for polystyrene which lacks a strong  $\gamma$  relaxation in an equal temperature span below its  $T_g$ . Increases in  $\alpha$  ( $= 3\alpha'$ ) well below  $T_g$ , which we associate with in-chain motion of  $(-\text{CH}_2-)_n$  moieties (with  $n \geq 3-5$ ), are considered responsible for the fact that literature values of  $\alpha_g$  just below  $T_g$  for these three polymers are higher than the normal  $\alpha_g$  of  $2 \times 10^{-4} \text{ deg}^{-1}$  reported for many polymers such as polystyrene. DSC scans on Nylon 6,6 and the copolymer show no unusual features in the  $\gamma$  region.

One of us recently noted<sup>2a</sup> that values of the glassy state coefficient of cubical expansion,  $\alpha_g$  (measured just below the glass temperature,  $T_g$ ), were considerably above the normal value of about  $2 \times 10^{-4} \text{ deg}^{-1}$  for aliphatic nylons and ethylene-vinyl acetate (E-VAC) random copolymers. We proposed that these high values of  $\alpha_g$  were associated with the  $T < T_g$  or  $\gamma$  relaxation present in these polymers and copolymers and generally ascribed to motion of three to five in-chain methylene groups.<sup>2b,3</sup> We postulated the existence of discontinuities in thermal expansion at  $T_\gamma$  from this in-chain motion, in analogy with discontinuities in  $\alpha$  found by Simha and his colleagues for side-chain motion in the alkyl methacrylate<sup>4,5</sup> and alkyl vinyl ether<sup>6,7</sup> families of polymers.

Since this postulate was crucial in our attempt<sup>2a</sup> to understand the glass transition and thermal expansion behavior of polyethylene, some experimental verification seemed desirable. The linear variable differential transformer technique, LVDT, used extensively by Simha and his collaborators<sup>4-8</sup> is ideally suited for the temperature range of most interest, namely, from liquid nitrogen to the glass temperature. It is also used down to liquid helium temperatures. Our materials were also examined in the latter range but these results will be reported elsewhere as part of a master's thesis by one of us.<sup>9</sup>

The aliphatic nylons and E-VAC copolymers can be written generically as containing the moiety,  $-\text{R}-(\text{CH}_2)_n-\text{R}-$ , with appropriate values of R. We<sup>2a</sup> assumed them to be ideal model compounds for studying the glass transition phenomena in polyethylene for two reasons. (1) They have relatively unambiguous glass transitions which decrease with  $n$ , in addition to a  $\gamma$  relaxation around  $150^\circ\text{K}$  whose temperature is approximately independent of  $n$ , al-

(1) (a) Department of Macromolecular Science; (b) The Dow Chemical Co.

(2) (a) R. F. Boyer, *Macromolecules*, **6**, 288 (1973); (b) A. H. Willbourn, *Trans. Faraday Soc.*, **54**, 717 (1958).

(3) F. P. Reding, J. A. Faucher, and R. D. Whitman, *J. Polym. Sci.*, **57**, 483 (1962).

(4) R. A. Haldon and R. Simha, *J. Appl. Phys.*, **39**, 1890 (1968).

(5) R. A. Haldon and R. Simha, *Macromolecules*, **1**, 340 (1968).

(6) R. A. Haldon, W. J. Schell, and R. Simha, *J. Macromol. Sci. Phys.*, **1**, 759 (1967).

(7) W. J. Schell, R. Simha, and J. J. Aklonis, *J. Macromol. Sci. Rev. Macromol. Chem.*, **3**, 1297 (1969).

(8) J. L. Zakin, R. Simha, and H. C. Hershey, *J. Polym. Sci.*, **10**, 1455 (1966).

(9) S. Lee, Department of Macromolecular Science, Case-Western Reserve University.